

GaSb-, InGaAsSb-, InGaSb-, InAsSbP- and Ge-TPV cells for low-temperature TPV applications

Oleg V. Sulima^{1*}, Andreas W. Bett², Michael G. Mauk¹, Frank Dimroth², Partha S. Dutta³, and Robert L. Mueller⁴

¹*AstroPower Inc., Solar Park, Newark, Delaware 19716-2000, USA*

²*Fraunhofer Institute for Solar Energy Systems, Heidenhofstrasse 2, D-79110 Freiburg, Germany*

³*Rensselaer Polytechnic Institute, Troy, New York 12180-3590, USA*

⁴*Jet Propulsion Laboratory, 4800 Oak Grove Drive, Pasadena, California 91109-8099, USA*

*corresponding author: sulima@astropower.com, phone: 302-366-0400 ext. 3031, fax: 302-283-0162

Abstract. GaSb thermophotovoltaic (TPV) cells are the most suitable choice for modern TPV generators, both in terms of efficiency and simplicity of the diffusion technology used. Actually, TPV generators based on GaSb solar cells are the only ones available on the market. However, TPV cells with band gaps (E_g) lower than GaSb are expected to be advantageous for low-temperature ($< 1000^\circ\text{C}$) non-wavelength-selective TPV radiators because they provide more effective absorption of the blackbody infrared radiation. In this work, together with GaSb ($E_g = 0.72$ eV), semiconductors with a lower E_g - Ge ($E_g = 0.66$ eV), InGaSb ($E_g = 0.60$ eV), InGaAsSb ($E_g = 0.55$ eV) and InAsSbP ($E_g = 0.39$ eV) - were studied for TPV cells. InGaAsSb cells seem to be the most promising candidate to replace GaSb cells in the low-temperature TPV generators.

INTRODUCTION

A simple and economic “no-epitaxy” technology of GaSb TPV cells using Zn diffusion from the vapor phase has proven to be suitable for production. Currently, only TPV generators based on GaSb solar cells are available on the market [1].

Nevertheless, materials with band gaps lower than GaSb are desirable for low-temperature ($< 1000^\circ\text{C}$) non-wavelength-selective TPV radiators. Therefore, in this work, together with GaSb ($E_g = 0.72$ eV), semiconductors with a lower E_g - Ge ($E_g = 0.66$ eV), InGaSb ($E_g = 0.60$ eV), InGaAsSb ($E_g = 0.55$ eV) and InAsSbP ($E_g = 0.39$ eV) - are studied for TPV cells.

To form pn-junctions in III-V materials, we used the most simple and productive method – low-temperature (from 340°C for InAsSbP to 480°C for GaSb) pseudo-closed-box Zn diffusion from the vapor phase. One-layer n-type epitaxial structures were grown by liquid phase epitaxy prior to the Zn diffusion only in the case of InGaAsSb and InAsSbP.

Further ways to simplify the technology of III-V TPV cells and reduce their price include using polycrystalline substrates and/or ternary substrates such as InGaSb. In

this work, a first attempt to fabricate an InGaSb TPV cell from a polycrystalline boule material was made.

It was determined that a careful optimization of the Zn diffusion profiles in TPV cells leads to a significant improvement of device performance [2,3]. The formation of strong built-in electrical fields near the emitter surface provides a dramatic decrease in the surface recombination losses. Thus high-efficiency TPV cells can be fabricated without any passivating window.

The main obstacle to the large-scale application of III-V TPV cells is the high cost of III-V substrates (including polycrystalline). Ge TPV cells made on substrates that are 6-7 times less expensive than those of GaSb, can be a cost-effective alternative to III-V cells. In this work, Ge cells were fabricated using diffusion of P into p-type substrates.

EXPERIMENTAL

TPV cells based on single crystal GaSb, InGaAsSb, InAsSbP and Ge, as well as on polycrystalline GaSb and InGaSb structures fabricated at Fraunhofer ISE, AstroPower and RPI were tested at Fraunhofer ISE and JPL.

A schematic of a TPV cell with a diffused emitter investigated in this work is presented in Figure 1. Description of the cell parts is given in Table 1.

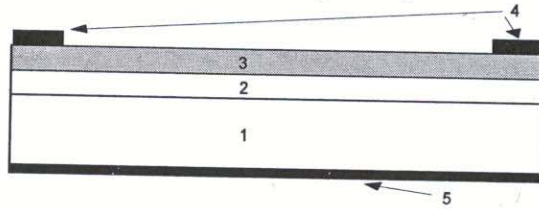


FIGURE 1. Scheme of TPV cells with a diffused emitter investigated in this work. Description of the cell parts is given in the Table 1. Numbers refer to column 1 of Table 1. Different contact grid designs used in this work are described in [4].

TABLE 1. Materials used for different parts of the studied TPV cells.

Part of the cell	GaSb-cell	InGaSb-cell	InGaAsSb-cell	InAsSbP-cell	Ge-cell
1. Substrate	n-GaSb single and polycrystalline	n-InGaSb polycrystal- line	n-GaSb single crystal	n-InAs single crystal	p-Ge single crystal
2. Epitaxial base	none	none	n-InGaAsSb	n-InAsSbP	none
3. Diffused emitter	p-GaSb	p-InGaSb	p-InGaAsSb	p-InAsSbP	n-Ge
4. Front side contact	Ti/Ni/Au				Ni/Au-Ge
5. Backside contact	Au-Ge				Ti/Pd/Ag

Details of the Zn diffusion process applied for III-V cells are published in Ref. [5]. Liquid phase epitaxy is used to grow base n-InGaAsSb or n-InAsSbP layers. Details of the epitaxial growth are described elsewhere [6].

Diffused n-type emitters in p-Ge ($p = 3\text{--}5 \times 10^{17} \text{ cm}^{-3}$) substrates are formed through diffusion of phosphorus. Two different methods of phosphorus diffusion are used: (i) diffusion during the MOCVD growth of InGaP on Ge, and (ii) diffusion from phosphorus spin-on dopants. In the case of method (i) the epitaxial InGaP layer is selectively removed from the Ge substrate after the diffusion. Method (i) in comparison with method (ii) seems to be too complicated. However, InGaP/Ge structures may be available as a sub-product of multi-junction solar cell fabrication.

Carrier concentration in Ge was measured by electrochemical CV profiling. Figure 2 shows the carrier concentration profile of a Ge cell that exhibited the best device parameters in this work (see below).

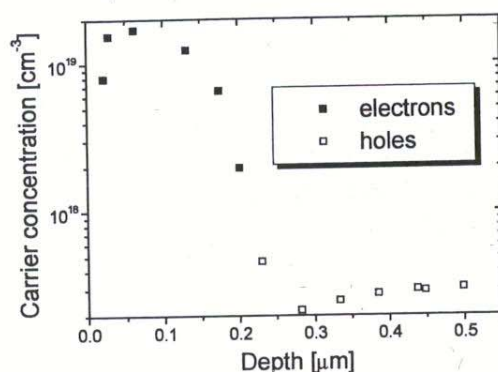


FIGURE 2. Carrier concentration profile in the Ge cell considered in this work. The profile is measured by electrochemical CV-profiling.

RESULTS AND DISCUSSION

Figure 3 shows the external quantum efficiency (EQE) spectra of a typical GaSb TPV cell together with other single crystal and polycrystalline TPV cells studied in this work.

The larger the long wavelength sensitivity of the TPV cell, the lower can be the radiator temperature. Hence if one considers only the photosensitivity range, InAsSbP cells with their sensitivity up to 3500 nm look to be the most promising for the low-temperature TPV generators. However, decrease of the bandgap inevitably causes reduction of the generated voltage. Thus, a trade-off between the increasing current and falling voltage must be found. Regarding the InAsSbP cells, problems with achieving sufficient voltage and FF impede their application. The open-circuit voltage (V_{oc}) achieved in these cells has been limited to about 0.1 V both in the cells with epitaxial [7] and diffusion emitters (this work).

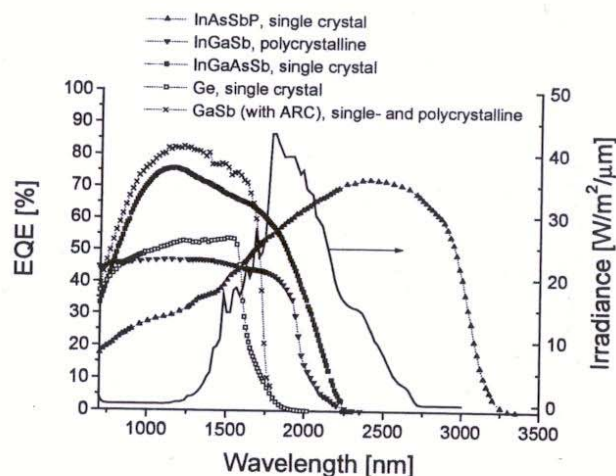


FIGURE 3. External quantum efficiency spectrum of the TPV cells (long wavelength part) measured in this work. Antireflection coating (anodic oxide) was applied only to the GaSb cell. Shadowing losses caused by the contact grid were within 15-20%. The spectrum of the JPL IR bandpass filtered large area pulsed solar simulator (LAPSS) irradiance (solid line, right axis) is shown for comparison.

Thus, the ratio between V_{oc} and the potential difference at the pn-junction in the used InAsSbP ($E_g = 0.39$ eV) is only 0.25. It is noteworthy that nearly the same low voltages (0.12 V) were observed in polycrystalline InGaSb cells, where the above mentioned ratio was even lower: 0.20. For comparison, this ratio equals 0.5 - 0.6 in GaSb and InGaAsSb. One can assume that it is the surface leakage that prevents obtaining a V_{oc} of around 0.2 V in InAsSbP. In the case of the polycrystalline InGaSb, both the surface and the bulk can cause the reduced voltage.

Let us now consider the InGaAsSb cell that has the next longest wavelength response up to 2250 nm (Fig. 3). In contrast to the InAsSbP cell, relatively high voltages were achieved in such a cell using an optimized diffused emitter [2]. Thus as shown below, InGaAsSb is a very promising candidate to replace GaSb in the low-temperature TPV applications.

Device parameters of GaSb, InGaAsSb and Ge TPV cells were measured under different illumination conditions including the JPL IR bandpass filtered large area pulsed solar simulator (LAPSS). The spectrum of the filtered LAPSS irradiance is shown in Figures 3 and 6. Output electric power densities of the measured devices is shown in Figure 4. The InGaAsSb cell demonstrated a superior performance under the LAPSS illumination. Ge cells showed the worst EQE (Fig. 3) and thus the lowest current. The voltage of Ge cells was relatively poor as well (Fig. 5) - lower than of the InGaAsSb ones despite the higher bandgap of Ge.

Concerning the LAPSS measurements one should note the following. It is clear from Figure 6, that even the blackbody spectrum ($T = 1610$ K, 3206-fold attenuated) that is the closest to the LAPSS spectrum does not match it very closely. That is the

reason why additional calculations of the output power were performed for different blackbody spectra.

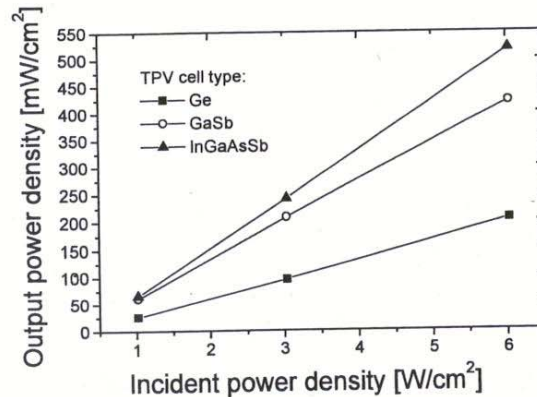


FIGURE 4. Output power density of Ge, GaSb and InGaAsSb TPV cells measured with the JPL LAPSS at different incident power densities at a cell temperature of 30°C.

Experimentally determined IV-characteristics and EQE-spectra allow an accurate calculation of TPV cell performance for any blackbody illumination at any temperature. Figure 7 shows the calculated output power of GaSb and InGaAsSb TPV cells as a function of the blackbody temperature. Taking into account optical losses in a TPV system, we assumed that the blackbody illumination of the cell is "scaled" (its intensity at all wavelengths is proportionally reduced). The scaling factor was assumed to be 0.6. Figure 7 shows that the low bandgap InGaAsSb TPV cells are advantageous for low radiator temperatures if no filters or selective emitters are used. For example, at $T = 973\text{K}$ the output power of the InGaAsSb cell is 1.6 times higher than that of the GaSb one.

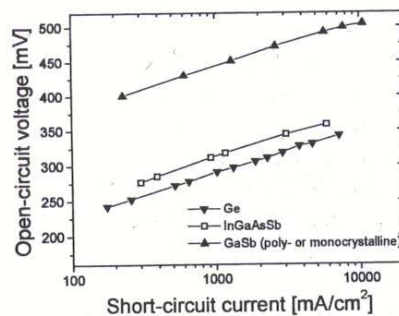


FIGURE 5. Open-circuit voltage of Ge, InGaAsSb and GaSb TPV cells vs. short-circuit current at 25°C.

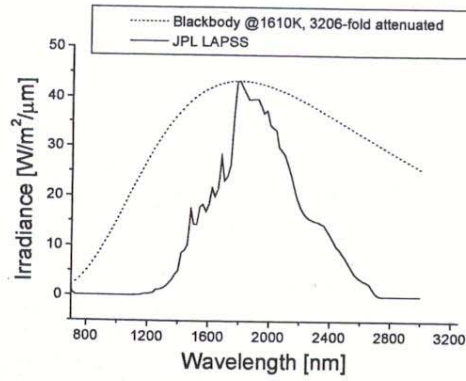


FIGURE 6. Comparison of the JPL LAPSS spectrum with the closest fit attenuated blackbody 1610 K spectrum.

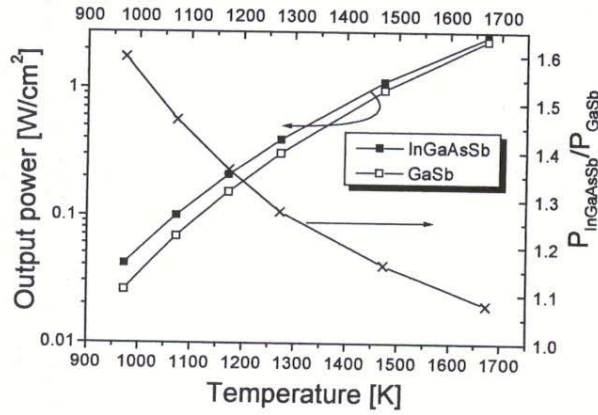


FIGURE 7. Calculated output power density of GaSb and InGaAsSb TPV cells as a function of blackbody temperature for the blackbody spectra with a scaling factor of 0.6. The calculations are performed for a cell temperature of 25°C and are based on measured device parameters (EQE, V_{oc} , FF). The ratio between the output power generated in the InGaAsSb and GaSb cells is shown on the right axis.

It is commonly believed that TPV cells operate at elevated temperatures. In this work, we determined temperature coefficients (TC) of short-circuit current (I_{sc}), V_{oc} , FF of GaSb, InGaAsSb and Ge cells using the JPL LAPSS. As the bandgap of semiconductors decreases with temperature, the spectral range of the photosensitivity widens into the long wavelength part. It is the prime reason why the TC of I_{sc} is usually positive. However, the exact value of the TC of I_{sc} is dependent on illumination spectrum and thus can be used only for the relative and not absolute cell comparison. TCs of V_{oc} and FF are not spectrum dependent and can be compared with the results of

other authors. Table 2 shows the absolute and relative temperature coefficients of V_{oc} and FF at different LAPSS illumination.

TABLE 2. Absolute and relative temperature coefficients of V_{oc} and FF at different LAPSS illumination.

Incident power density Cell material	$P_{inc} = 1021 \text{ mW/cm}^2$	$P_{inc} = 3037 \text{ mW/cm}^2$	$P_{inc} = 6029 \text{ mW/cm}^2$
Open-circuit voltage (V_{oc})			
InGaAsSb	- 1.525 mV/°C - 0.49 %/°C	- 1.496 mV/°C - 0.43 %/°C	- 1.465 mV/°C - 0.40 %/°C
GaSb	- 1.687 mV/°C - 0.39 %/°C	- 1.672 mV/°C - 0.36 %/°C	- 1.620 mV/°C - 0.33 %/°C
Ge	- 1.877 mV/°C - 0.67 %/°C	- 1.916 mV/°C - 0.62 %/°C	- 1.913 mV/°C - 0.59 %/°C
Fill factor (FF)			
InGaAsSb	- 0.00079 /°C - 0.13 %/°C	- 0.00108 /°C - 0.17 %/°C	- 0.00128 /°C - 0.19 %/°C
GaSb	- 0.00102 /°C - 0.15 %/°C	- 0.00155 /°C - 0.22 %/°C	- 0.00216 /°C - 0.31 %/°C
Ge	- 0.00268 /°C - 0.39 %/°C	- 0.00280 /°C - 0.41 %/°C	- 0.00254 /°C - 0.41 %/°C

The lowest absolute and relative TCs of V_{oc} were determined at $P_1 = 6 \text{ W/cm}^2$: - 1.465 mV/°C (in InGaAsSb-cells) and -0.33 %/°C (in GaSb-cells), respectively. The lowest absolute and relative TCs of FF were measured in InGaAsSb-cells at $P_1 = 1 \text{ W/cm}^2$: -0.00079 /°C and 0.13 %/°C, respectively. TCs of V_{oc} and FF in Ge-cells were essentially worse.

CONCLUSIONS

Device parameters of GaSb-, InGaAsSb-, InGaSb-, InAsSbP- and Ge- TPV cells were compared. GaSb- and InGaAsSb- based TPV cells showed the best performance.

Compared to GaSb, InGaAsSb cells demonstrated better parameters when measured under the JPL LAPSS or calculated on the basis of experimental results. The advantage of InGaAsSb cells is especially large if low-temperature blackbody radiators without filters are used.

Although Ge TPV cells exhibit lower efficiencies and worse temperature characteristics than GaSb and InGaAsSb ones, the relatively low cost of Ge may still make TPV Ge cells attractive.

Polycrystalline InGaSb- and single crystal InAsSbP-based cells demonstrated high photocurrent. However, their voltage and FF need to be improved.

ACKNOWLEDGEMENTS

The authors wish to thank J. Cox from AstroPower for epitaxial growth of quaternary alloys, E. Schaeffer, R. Beckert, G. Siefer, Klaus Breithaupt and H. Lautenschlager from Fraunhofer Institute for Solar Energy Systems for assistance by fabrication and testing of TPV cells, and P. Sims from AstroPower for useful discussions.

REFERENCES

1. www.realgoods.com/renew/shop/product.cfm?dp=1000&sd=1006&ts=3006374
2. Sulima, O.V., Beckert, R., Bett, A.W., Cox J.A., and Mauk, M.G., IEE Proc.-Optoelectron., 147, 199-204 (2000).
3. Sulima, O.V., and Bett, A.W., Solar Energy Materials & Solar Cells, 66, 533-540, 2001.
4. Bett, A.W., Keser, S., Stollwerck, G., and Sulima, O.V., "Large-Area GaSb Photovoltaic Cells", in Thermophotovoltaic Generation of Electricity -1997, edited by T.J. Coutts et al., AIP Conference Proceedings 401, American Institute of Physics, New York, pp. 41-53.
5. Sulima, O.V., Bett, A.W., Mauk, M.G., Ber, B.Ya., and Dutta, P.S., "Diffusion of Zn in TPV materials: GaSb, InGaSb, InGaAsSb and InAsSbP", this conference.
6. Mauk, M. G., Shellenbarger, Z. A., Cox, J. A., Sulima, O.V., Bett, A.W., Mueller, R. L., Sims, P. E., McNeely, J. B., DiNetta, L. C., J. of Cryst. Growth, 211, 189-193 (2000).
7. Mauk, M.G., Shellenbarger, Z.A., Cox, J.A., Tata, A.N., Warden, T.G., and DiNetta, L.C., "Advances in low-bandgap InAsSbP/InAs and GaInAsSb/GaSb thermophotovoltaics", in Proceedings of the 28th IEEE Photovoltaic Specialists Conf., 2000, pp. 1028-1031.